

Numerical Simulation of Convective Combustion of Ball Powders in Strong Confinement

K. Kim*

Naval Surface Weapons Center, Silver Spring, Maryland

Efforts to simulate two-phase (solid and gas) convective combustion process of ball powders in strong confinement are described. Important constitutive mechanisms of the process and past efforts to simulate these mechanisms are explained. Results of the current effort, a parametric study of the process with varying ignition temperature, indicate that values of commonly accepted ignition temperatures as an ignition criterion may not be acceptable under high heat flux conditions of the convective combustion process. They also show, for the first time, that solid compaction wave is generated and moves ahead of the flame front at a higher velocity.

Introduction

THE ability of an energetic material (explosive or propellant) to undergo a transition to detonation from a burning mode is a fundamental and important characteristic of that material. In the absence of a fuze malfunction, a gun premature results from the ignition of the explosive fill by the confined burning (deflagration) of the explosive charge. Ignition of the explosive fill can lead to damage ranging from minor malfunctions to jamming of the shell in the barrel and destruction of the barrel by subsequent detonation. Also, experience shows that detonation may occur in high energy propellant motors due to a ballistic malfunction which produces granulation of the propellant. Burning in the granulated bed may lead to formation of a shock which initiates a transition to detonation.

A two-phase (solid and gas) convective combustion process has been observed to be an important first step of the deflagration-to-detonation transition (DDT) of porous energetic materials.^{1,2} One of the accepted scenarios³ on how the DDT progresses is as follows. Most experimental studies of DDT utilize an ignitor mixture to start the burning of the energetic material. The ignitor usually produces hot particles and/or hot combustion gases which lead to the ignition and confined burning of the energetic materials. In the preignition period, the hot gases from the burning of the ignitor can lead to compaction of the porous column of energetic material. In addition, pyrolysis of the material, which leads to ignition, will occur to some unknown extent. Once ignition of the energetic material occurs, then the confined burning produces combustion gases, increasing gas pressure in the ignitor region. The pressure gradient created pushes additional hot gases into voids of the neighboring area. If the gas pressure gradient is large enough, significant additional compaction of the porous bed may occur. At the same time, the pore walls are heated by the hot gases passing over them. If the heating is sustained, it may ignite the propellant *within* the bed. The additional ignited propellant joins the original propellant in further pressurization of the bed. Since burning rates of most propellants strongly depend on gas pressure, the sequence of events described above (gas generation, pressurization, gas

penetration, heat transfer, further ignition and burning) augments pressure buildup. This convective combustion continues until the confining structure ruptures as a result of the pressure buildup or shock-to-detonation transition (SDT) is obtained. SDT occurs when a series of compressive waves in the porous solid emanating from the region of convective combustion coalesce into a strong shock, starting a chemical reaction at a location sometimes far away from the location of original convective combustion. Accurate understanding of convective combustion is necessary to determine the shock characteristics as well as its location.

Theoretical understanding and development of a physical model of the DDT are difficult due to the complexity of the process. Many constitutive factors play important roles in the course of the DDT process. They interact with each other in a nonlinear fashion. Due to the lack of an accurate description of the constitutive factors, earlier modeling efforts^{4,5} were limited in their scopes. Descriptions of the ignitor gas generation rate and the compaction of reactive materials in these models were arbitrarily chosen. Also, the convective combustion was assumed to take place at the location where SDT occurs. However, there is experimental evidence⁶ that indicates that the gas pressure may not be significant at the location where the transition process occurs.

It is the object of this paper to present results of numerical simulation of the onset of convective combustion with the minimum amount of uncertainty associated with the constitutive factors of the DDT process. The efforts were concentrated on observing parametric behavior of the convective combustion on one parameter, an ignition temperature. It is ultimately desired to determine if a solid compaction wave, running away from the flame front, is responsible for the formation of the shock wave that produces the transition to detonation. However, the actual transition process is not included in the paper.

Model Description

A laboratory scale experimental setup, a DDT tube designed by Sandusky and Bernecker was selected as the basis of the numerical simulation. Details of the setup are described elsewhere^{6,7}; only a brief sketch is given here. Varying sizes of powders of propellants or explosives are packed into a long tube, at different porosities, made of either plastic or steel. Both ends of the tube are closed, and a small amount of ignitor is located at one end. Events after the ignition of the ignitor are recorded by varying combinations of conducting pins, strain gages, pressure transducers, a framing camera, and flash radiography. Further explanations of the experiment to be simulated will follow later.

Presented as Paper 82-0356 at the AIAA 20th Aerospace Sciences Meeting, Orlando, Fla., Jan. 11-14, 1982; submitted Jan. 22, 1982; revision received July 17, 1983. This paper is declared a work of the U.S. Government and therefore is in the public domain.

*Mechanical Engineer, Detonation Physics Branch. Currently, visiting Professor at Korea Advanced Institute of Science and Technology, Seoul, Korea.

In order to simulate the convective combustion process, a one-dimensional, two-phase (gas and solid), reacting flow computer code developed to model gun interior ballistics was modified. This choice was made because there are a number of similarities between interior gun ballistics and DDT. The similarities include: ignition and combustion of solids (explosives or propellants) due to heating from ignitor product gas, filtration of the combustion gas into a porous solid medium, and convective heating and compressive wave propagation in both gas and solid phases. Among existing gun interior ballistics codes, NOVA⁸ was selected. Other codes were compared by Kuo.⁹ The NOVA code is among the most advanced in programming and documentation. The code has been modified to accommodate different constitutive relations and numerical severities imposed by the high rate, high pressure DDT processes. The modified code, called DETOVA, which is derived from detonation and NOVA code, will later include such physical processes as SDT.

The DETOVA code considers a number of mixture regions, each containing both gas and solid, in a closed one-dimensional tube. The state of variables in each mixture region is solved by integrating nonlinear differential equations describing conservation of mass, momentum, and energy for both phases. The differential equations are coupled together by empirical correlations for 1) friction and heat transfer between the two phases, 2) an ignition criterion based upon surface temperature for the solid, and 3) burning rates for ignited solid. The equation of state used for the gas phase was the Noble-Abel equation⁸; that for the solid phase came from the quasistatic compaction experiments. A parametric study of the above empirical correlations and other physical parameters such as ignitor size, particle size of the solid material in the porous bed, and initial bed porosity identified the important parameters in the DDT process: the gas generation rate from the energetic material in the porous bed (ignition, burning rate, and available surface area for burning), the compaction of the porous bed, and the gas generation rate of the ignitor. Further details on the DETOVA code are available in Ref. 10.

Selection of Test Case

The numerical simulation is based upon experimental data obtained by Bernecker et al.¹¹ for various double-base powders. In particular, the DDT experiment selected used Olin TS3659 ball powder with an average particle size of 435 μm . The powder was packed into a steel tube to give a porous column of 60.4% theoretical maximum density. The steel tube was chosen because it provides stronger confinement than a Lexan tube. The problem becomes complex if the tube expands and an annular gap is created between the inner tube

wall and the solid bed. The tube deformation has been ignored in the analysis to maintain one-dimensionality of the problem.

There are many advantages to the selection of the ball powders. First, the average particle size is large enough to permit a relatively fast computation. For small particle sizes of reactive materials, time steps for computation need to be kept small to insure numerical stability. Second, the ball powders are tough and do not easily break into smaller particles during the early phases of the convective combustion, allowing a fairly accurate description of the available surface area. Third, their burning rate is known.¹² In the simulation, it was represented by

$$\dot{r} = 0.129p^{1.0} \quad (1)$$

where \dot{r} is the linear regression rate in cm/s and p is pressure in MPa. Also, erosive burning effects have been included. Fourth, the initial porosity (39.6%) of the ball powders is in the same range of porosities where the flow resistance law¹³ and the interphase heat transfer law¹⁴ have been obtained. This gives one confidence in the constitutive laws used in the convective combustion simulations. Last, one may estimate the static compaction behavior of the ball powders. Elban¹⁵ reported the static compaction behaviors of two of them, Olin WC140 (0% NG content) ball powders and Olin TS3660 (12.3% NG content) ball powders. Considering that the Olin TS3659 ball powders contain about 21% of NG and that the static compaction behaviors of WC140 and TS3660 are only slightly different, the static compaction behavior of TS3659 is assumed to be close to that of TS3660. In the simulation, the static compaction law was approximated by

$$\ln \sigma = 7.77 - 14.5 \times \epsilon + \frac{0.0001}{(\epsilon - 0.1)^2} \quad (2)$$

where σ is the intergranular stress in MPa and ϵ is the porosity. Therefore, $1 - \epsilon$ is the theoretical maximum density (TMD). Here σ is defined as:

$$\sigma = (1 - \epsilon)\tau_i$$

where τ_i is the intragranular stress given by Elban. The third term on the right-hand side of Eq. (2) was introduced as a convenient measure to prevent the compaction of ball powders below 10% porosity and thus to prevent numerical difficulties associated with low-porosity two-phase flow calculations. Errors introduced into the simulation of heat transfer and drag by this measure were not assessed due to lack of further information.

Experimental Record

Unfortunately, only a small amount of detailed information can be obtained from the steel tube experiment. Figure 1 shows the distance-time plot. The initial response of one of two optical fiber/photocell (OF/PC) assemblies by the ignitor gas serves as the time origin. Thereafter, the responses of the conductivity and ionization pins show the development of a strong compressive wave into a detonation at the location of 199 mm. The onset of convective combustion in the early portion of the DDT process is poorly defined because of the paucity of probe data. However, qualitative information about the earlier stages of the DDT process may be inferred from parallel studies in low confinement plastic tubes.¹¹

First, a weak compaction wave traveling at a speed of 0.35 ~ 0.45 m/ μs emanates at early times from the ignitor region. This weak compaction wave may be coming from the action of the ignitor gas on the ball powder bed. As the ball powders are ignited, the ignition front (or the flame front) propagates downstream at a lower speed. This generates additional gas which raises the pressure of the bed, compacting the ball powder bed further. A stronger compaction

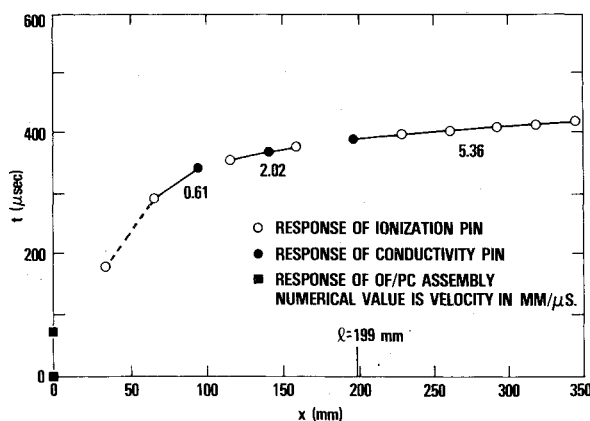


Fig. 1 Distance-time data from steel tube arrangement with Olin 3659 (21.6% NG) ball powder, 0.99 g/cm³.

wave is expected to emerge upstream, ahead of the flame front, traveling at a faster velocity than the flame front and the weak compaction front. The flame front velocity is expected to be of the order of 0.2 mm/ μ s or lower. In the simulation, this qualitative description will be examined as the primary checkpoint.

Simulation

Parameters used in the simulation are listed in Table 1. The ignitor gas generation rate was obtained from results of candidate dynamic compaction experiments with inert materials (melamine and Teflon) whose static compaction behaviors are known.¹⁶ The selected ignitor gas generation rate simulated all of the candidate dynamic compaction experiments satisfactorily. The ignitor used in the simulation was packed in a circular disk 1.73 mm high by 25.4 mm in diameter with an average particle size of 140 μ m and a packing density of 51.2% TMD. Particles are assumed to be spherical in shape and the whole surface area is assumed to burn once ignited. The ignitor is assumed to have been ignited at the start of simulation and to burn at the rate given above. In addition, a small ignitor gas source is assumed to exist which sends out gas at a rate of 0.79 g/ms for the first 0.28 ms. The total amount of gas is about 0.82 g, which is close to the ignitor mass in the experiments. See Ref. 16 for further details.

Boggs et al.¹⁷ showed that the gas phase chemical kinetics, which are normally ignored in the study of ignition temperature at low heat flux levels, becomes such a dominant factor at higher heat flux levels ($> 2 \sim 300$ cal/cm²s) that the concept of ignition temperature is questioned. The validity of

the use of a single-step chemical reaction is also questioned at the high heat flux levels. One may have to consider chemical reactions in various phases (gas, solid, and interface) occurring in three-dimensional geometry (in bed interstices) dictated by local flow conditions. However, this is difficult at the present time. An alternative approach is taken for the ignition and combustion of the ball powders at high heat flux levels. That is, single-step chemical reaction is still assumed, but the ignition temperature is artificially raised to accommodate the delay of the ignition caused by gas phase chemical reactions. The value of the ignition temperature is unknown. In this paper, several different values of the ignition temperature have been tried to observe a parametric behavior of convective combustion, rather than a definite simulation of the given experiment. The ignition temperatures tried were 556, 667, 778, and 889 K.

Results

Loci of the flame front and the compaction wave front calculated with above parameters are plotted in the time-distance plot shown in Fig. 2. The figure shows that with the ignition temperature of 556 or 667 K, the flame front propagates so fast that the solid compaction wave cannot run away from it. That means the ignition of ball powders is so fast that the flame penetration into the porous bed is faster than or at least equal to the solid compaction wave propagation. Considering that there is not much gas in the vicinity of the location where the transition to detonation occurs,⁶ one concludes that this is not realistic.

If the ignition temperature is 778 or 889 K, the convective ignition process is sufficiently slow that solid compaction waves propagating ahead of the flame front are observed. One is the weak compaction wave whose front is defined to be where the solid stress becomes larger than the magnitude achieved by a passage of an elastic precursor wave (~ 14 MPa in the test case). Its propagating velocities are 0.41 and 0.43 mm/ μ s, showing good agreement with the experimentally deduced velocity of 0.35 \sim 0.45 mm/ μ s.

The other is the strong compaction wave whose amplification and acceleration eventually overtake the front running weak compaction wave and leads to SDT. In this paper, only the early part of the strong compaction wave is shown.

The calculated flame front velocity (0.23 or 0.33 mm/ μ s) is higher than expected. This may indicate that the ignition temperature used is still too low.

Overall, with the exception of the magnitude of the flame front velocity, the general features of the early phase of the convective combustion described earlier are reproduced in the simulation. It is of interest now to study the details of the flow

Table 1 Input parameters

Length of the DDT tube	22.9 cm
Number of computational cells	41
Initial ambient gas	
Temperature	21°C
Pressure	0.1 MPa
Molecular weight	24.1 g/mole
Ratio of specific heats	1.33
Solid	
Initial temperature	21°C
Material and initial density	60.4% TMD Olin TS 3659 ball powder
Grain diameter	424 μ m, spherical
Compaction law	Eq. (2)
Ignition temperature	See text
Burning rate	Eq. (1) with erosive burning effect
Erosive burning preexponential factor	3.76 cm ³ K/J
Erosive burning exponential factor	105
Gas phase thermochemistry	
Heat of reaction	4.65 $\times 10^3$ J/g
Molecular weight	24.8 g/mole
Ratio of specific heats	1.227
Covolume	0.361 cm ³ /g
Thermal conductivity	1.0 $\times 10^{-3}$ cal/cm/s/k
Thermal diffusivity	0.2 $\times 10^{-2}$ cm ² /s
Ignitor	
Material	B/KNO ₃
Gas generation rate	See text with the burning rate below
Burning rate	2.67 $p^{0.107}$ cm/s (with p in MPa) with same erosive burning effect as ball powders
Gas phase thermochemistry	
Heat of reaction	2.21 $\times 10^3$ J/g
Molecular weight	66.8 g/mole
Ratio of specific heats	1.114
Covolume	0.0 cm ³ /g

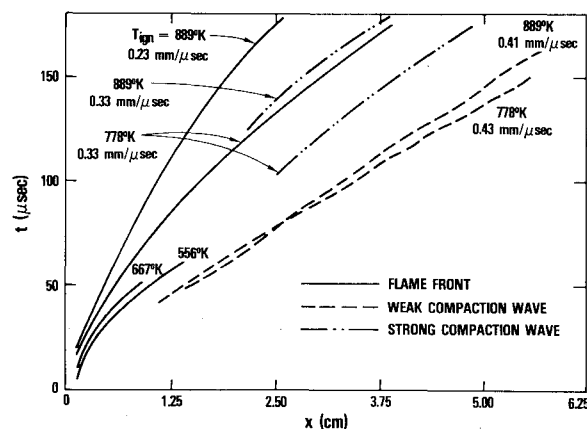


Fig. 2 Distance-time plots of flame front, weak compaction wave, and strong compaction wave. Velocities are taken at around 2.5 cm for each.

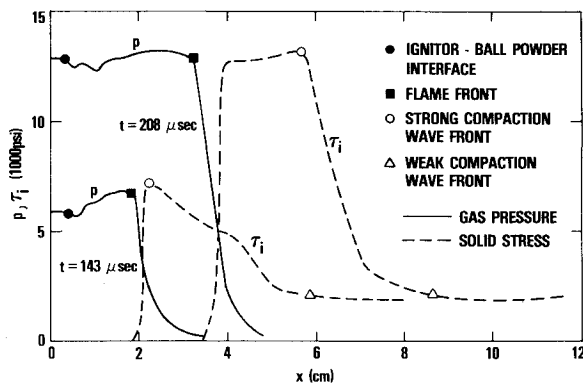


Fig. 3 Gas pressure and solid stress profiles.

to obtain more insight into the process. For this purpose, gas pressure (and solid stress)-distance profiles are generated at two different times for the case of $T_{\text{ign}} = 889 \text{ K}$ in Fig. 3. The solid curves represent gas pressure profiles at $t = 143$ and $208 \mu\text{s}$. The dashed curves represent solid stress profiles. At each time, the ignitor ball/powder interface, the flame front, the strong compaction wave front, and the weak compaction wave front are indicated. Several features can be noted. First, the ignitor ball/powder interface is almost standing still after an initial movement downstream. Second, the gas pressure behind the flame front is almost equilibrated in that space, but gas penetration downstream is a slow process producing a precipitous pressure drop in the downstream direction ($>4 \text{ cm}$ at $208 \mu\text{s}$), ahead of the flame front. Third, the ball powder bed is being compacted by the gas pressure gradient before it is ignited. Once a portion of the bed is ignited, it does not compact any further, dropping the intergranular stress to zero. Burning of the powders also acts to remove the intergranular stress. Fourth, one notices the beginning of amplification of the strong compaction wave as time increases.

Once again, the observations from Fig. 3 agree with expectations during the early convective combustion process. The gas penetration downstream is shown to be a relatively slow process. Unless the flame propagation fails entirely, the localization of gas pressure near the ignitor region will compact the ball powder bed, accelerating the weak and the strong compaction wave propagation downstream. This process is enhanced by formation of a low porosity plug (the region of high solid stress) ahead of the flame front which further reduces the gas penetration downstream.

Summary

A parametric study of numerical simulation of convective combustion has been presented and basic processes have been identified. The separation of the solid stress wave from the flame front has been observed numerically, paving the way for the introduction of shock-to-detonation transition into the

DETOVA code in order to accomplish deflagration-to-detonation transition simulation.

Acknowledgments

The author wishes to thank Dr. R. R. Bernecker and Dr. J. Short for their helpful discussions.

References

- 1 Bernecker, R. R. and Price, D., "Studies in the Transition from Deflagration-to-Detonation in Granular Explosives," II and III, *Combustion and Flame*, Vol. 22, 1974, pp. 119-129 and 162-170.
- 2 Belyaev, A. F., Bovolev, V. K., Korotkov, A. I., Sulimov, A. A. and Chuiko, S. V., *Transition from Deflagration to Detonation in Condensed Phases*, Israel Program for Scientific Translations, 1975.
- 3 Bernecker, R. R., Sandusky, H. W., and Clairmont, A. R. Jr., "Deflagration-to-Detonation Transition Studies of Porous Explosive Charges in Plastic Tubes," *Proceedings of the 7th Symposium on Detonation*, Naval Surface Weapons Center, NSWC MP 82-334, 1982.
- 4 Beckstead, M. W., Peterson, N. L., Pilcher, D. T., Hopkins, B. D., and Krier, H., "Convective Combustion Modeling Applied to Deflagration-to-Detonation Transition of HMX," *Combustion and Flame*, Vol. 30, 1977, pp. 231-241.
- 5 Butler, P. B., Lembeck, M. F., and Krier, H., "Modeling of Shock Development and Transition to Detonation Initiated by Burning in Porous Propellant Beds," *Combustion and Flame*, Vol. 46, 1982, pp. 75-93.
- 6 Campbell, A. W., "Deflagration-to-Detonation Transition in Granular HMX," *Proceedings, 1980 JANNAF Propulsion Systems Hazards Subcommittee Meeting*, Vol. 1, 1980, pp. 105-130.
- 7 Sandusky, H. W. and Bernecker, R. R., "Transparent Tube Studies of Burning to Detonation Transition in Granular Explosives I: Preliminary Framing Camera Studies," Naval Surface Weapons Center, NSWC TR 79-79, 1980.
- 8 Gough, P. S., "Numerical Analysis of a Two-Phase Flow with Explicit Internal Boundaries," Naval Ordnance Station, IHCR 77-5, 1977.
- 9 Kuo, K. K., private communication, 1977.
- 10 Kim, K., "Numerical Modeling of Deflagration-to-Detonation Transition in Granular Explosive Beds," Naval Surface Weapons Center, NSWC TR 80-437, to be published.
- 11 Bernecker, R. R., Clairmont, A. R., and Sandusky, H. W., private communication, 1981.
- 12 Price, C. F., private communication, 1981.
- 13 Kuo, K. K. and Nydegger, C. C., "Flow Resistance Measurements and Correlation in a Packed Bed of WC 870 Ball Propellants," *Journal of Ballistics*, Vol. 2, 1, 1978.
- 14 Denton, W. H., "The Heat Transfer and Flow Resistance for Fluid Flow Through Randomly Packed Spheres," *Journal of Mechanical Engineering*, 1951, pp. 370-373.
- 15 Elban, W. L., private communication, 1981.
- 16 Sandusky, H. W., Elban, W. L., Kim, K., Bernecker, R. R., Gross, S. B. and Clairmont, A. R., "Compaction of Porous Beds of Inert Materials," *Proceedings of 7th Symposium on Detonation*, Naval Surface Weapons Center, NSWC MP 82-334, 1982.
- 17 Boggs, T. L., Price, C. F., Atwood, A. I., Zurn, D. E., and Derr, R. L., "Role of Gas Phase Reactions in Deflagration-to-Detonation Transition," *Proceedings of the 7th Symposium on Detonation*, Naval Surface Weapons Center, NSWC MP 82-334, 1982.